Comparisons of Analog and Digital Impulse Radio for Wireless Multiple-Access Communications

Moe Z. Win and Robert A. Scholtz
Communication Sciences Institute
Department of Electrical Engineering-Systems
University of Southern California, Los Angeles, CA 90089-2565 USA

Abstract— **Attractive features of time-hopping spread-spectrum multiple access systems employing impulse signal technology are outlined and emerging design issues are described. Performance of such communications systems in terms of multiple-access capability is estimated for both analog and digital data modulation formats under ideal multiple access channel conditions.**

I. Introduction to Impulse Radio Systems

THE term *wideband*, as applied to communication systems, can have different meanings. When applied to conventional systems, it refers to the data modulation bandwidth. In that case, the more wideband a system is, the higher its data transmission rate. In this paper, a spread-spectrum system [1], [2] is described in which the transmitted signal, even in the absence of data modulation, occupies an extremely large bandwidth. In this case, with a fixed data modulation rate, as the transmitted signal bandwidth increases, the signal may become more covert because its power density is lower, may have higher immunity to the effects of interference, and may have improved time-of-arrival resolution.

The spread-spectrum radio system described here is unique in another regard: It does not use sinusoidal carriers to raise the signal to a frequency band in which signals propagate well, but instead communicates with a time-hopping baseband signal composed of subnanosecond pulses (referred to as *monocycles*). Since its bandwidth ranges from near d.c. to several GHz, this *impulse radio* signal undergoes distortions in the propagation process, even in very benign propagation environments. On the other hand, the fact that an impulse radio system operates in the lowest possible frequency band that supports its wide transmission bandwidth, means that this radio has the best chance of penetrating materials that tend to become more opaque at higher frequencies.

Finally it should be noted that the use of signals with GHz bandwidths implies that multipath is resolvable down to path differential delays on the order of a nanosecond or less, i.e., down to path length differentials on the order of a foot or less. This significantly reduces fading effects, even in indoor environments, and the resulting reduction of fading margins in link power budgets leads to reduced transmission power requirements.

The modulation format described in this paper can be supported by current technology. The receiver processing and performance predictions, for both analog and digital data modulation formats, are considered under ideal multiple access channel conditions. Real indoor channel measurements and their implications for Rake receiver design [3]–[6]will be discussed in a sequel.

II. System Model

A. Time-Hopping Format Using Impulses

A typical time-hopping format employed by an impulse radio in which the $k^{\underline{\text{th}}}$ transmitter's output signal $s_{\text{tr}}^{(k)}(u, t^{(k)})$ is given by

$$s_{\text{tr}}^{(k)}(u, t^{(k)}) = \sum_{j=-\infty}^{\infty} w_{\text{tr}}(t^{(k)} - jT_{\text{f}} - c_j^{(k)}(u)T_{\text{c}} - d_j^{(k)}(u)),$$

where $t^{(k)}$ is the transmitter's clock time, and $w_{\text{tr}}(t)$ represents the transmitted monocycle waveform that nominally begins at time zero on the transmitter's clock.

The *frame time* or *pulse repetition time* T_{f} typically may be a hundred to a thousand times the monocycle width, resulting in a signal with a very low duty cycle. To eliminate catastrophic collisions in multiple accessing, each user (indexed by k) is assigned a distinct pulse shift pattern $\{c_j^{(k)}(u)\}$ called *time-hopping sequence*, which provides an additional time shift to each pulse in the pulse train. The $j^{\underline{\text{th}}}$ monocycle undergoing an additional shift of $c_j^{(k)}(u)T_{\text{c}}$ seconds, where T_{c} is the duration of addressable time delay bins. The addressable time-hopping duration is strictly less than the frame time since a short time interval is required to read the output of a monocycle correlator and to reset the correlator.

The sequence $\{d_j^{(k)}(u)\}_{j=-\infty}^{\infty}$ is a sample sequence from a wide-sense stationary random process $d^{(k)}(u, t)$, with samples taken at a rate of T_{f}^{-1}. Both analog and digital modulation formats are described in this paper. For the analog impulse radio, analog subcarrier signaling is considered where stabilization of tracking S-curve of the clock control

The research described in this paper was supported in part by the Joint Services Electronics Program under contract F49620-94-0022, and in part by the Integrated Media Systems Center, a National Science Foundation Engineering Research Center with additional support from the Annenberg Center for Communication at the University of Southern California and the California Trade and Commerce Agency.

The authors can be reached by E-mail at win@milly.usc.edu, scholtz@milly.usc.edu

loops can be accomplished with relatively simple receiver design. This signaling format is of particular interest for low power or miniaturized applications. For the digital impulse radio, a pulse position data modulation is considered. For simplicity, it is assumed that the data stream is balanced so that the clock tracking loop S-curve can maintain a stable tracking point. With more complicated schemes, pulse shift balance can be achieved in each symbol time.

B. The Multiple Access Channel

When $N_{\rm u}$ users are active in the multiple-access system, the composite received signal $r(u,t)$ at the output of the receiver's antenna is modeled as

$$r(u,t) = \sum_{k=1}^{N_{\rm u}} A_k s_{\rm rec}^{(k)}(u, t - \tau_k(u)) + n(u,t)\,,$$

in which A_k represents the attenuation over the propagation path of the signal $s_{\rm rec}^{(k)}(u, t-\tau_k(u))$ received from the $k^{\underline{\rm th}}$ transmitter. The random variable $\tau_k(u)$ represents the time asynchronisims between the clocks of transmitter k and the receiver and $n(u,t)$ represents other non-monocycle interferences (e.g., receiver noise) present at the correlator input.

The number of transmitters $N_{\rm u}$ on the air and the signal amplitudes A_k are assumed to be constant during the data symbol interval. The propagation of the signals from each transmitter to the receiver is assumed to be ideal, each signal undergoing only a constant attenuation and delay. The antenna modifies the shape of the transmitted monocycle $w_{\rm tr}(t)$ to $w_{\rm rec}(t)$ at the output of the receiver's antenna. A typical received pulse shape $w_{\rm rec}(t)$ is shown in Fig. 1. This channel model ignores multipath, dispersive effects, etc.

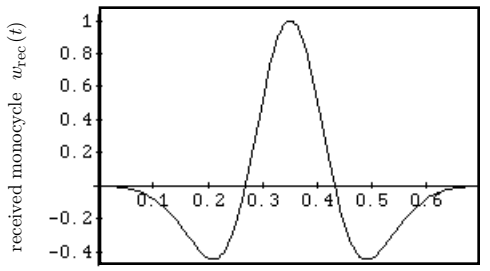

Fig. 1. A typical received monocycle $w_{\rm rec}(t)$ at the output of the antenna subsystem as a function of time in nanoseconds.

III. The Analog Impulse Radio Multiple Access Receiver

A. Signal Processing for the AIRMA Receiver

A simplified model describing a portion of the analog impulse radio multiple access (AIRMA) receiver is shown in Fig. 2. A more comprehensive description of the AIRMA receiver can be found in [7] where detailed calculations of the mathematical structure at various locations of the AIRMA receiver are made. The results are summarized along with important assumptions that were made during the calculations.

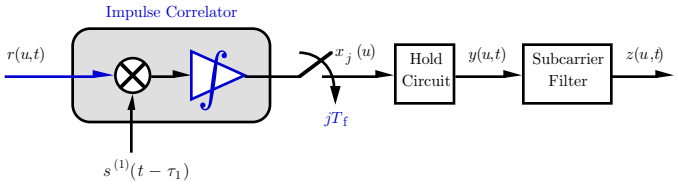

Fig. 2. Simplified model of the analog impulse radio multiple access receiver front end.

It is assumed that the receiver is locked-on to the transmission from the first user so that it achieves both clock and time-hopping sequence synchronization for that transmitted signal. Under the assumption of perfect signal reconstruction, the subcarrier filter output signal is evaluated in [8] as

$$z^{(1)}(u,t) = A_1 \widetilde{R}_w(d^{(1)}(u, t-\gamma')) \approx \dot{\widetilde{R}}(0) d^{(1)}(u, t-\gamma')\,, \tag{1}$$

where $\widetilde{R}_w(\tau)$ is the cross-correlation function of the received monocycle $w_{\rm rec}(t)$ and template generator output $w_{\rm cor}(t)$. The quantity $\dot{\widetilde{R}}(0)$ represents the slope of $\dot{\widetilde{R}}(t)$ at $t=0$, and γ' accounts for propagation and processing delays. The latter approximation in (1) is valid when the data modulation $d^{(1)}(u,t)$ is constrained to be within the linear region of the $\widetilde{R}(\cdot)$ function. Figure 3 shows exact and approximate expressions for the cross-correlation function $\widetilde{R}_w(\tau)$ for the typical received waveform given in Fig. 1.

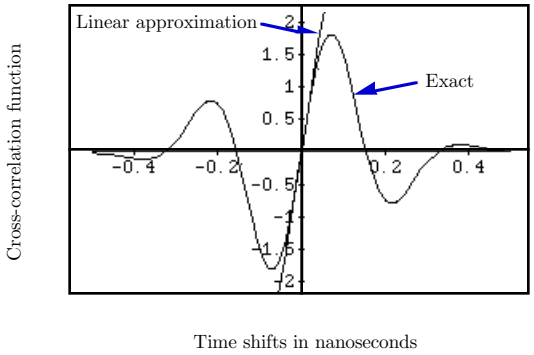

Fig. 3. Cross-correlation $\tilde{R}_w(\tau)$ between the received waveform and pulse correlator waveform. Also shown is the linear approximation of this cross-correlation function.

B. Signal-to-Noise Ratio of the AIRMA Receiver

Under the assumption of independent receiver noise samples, independent interference sources, and using random sequence selection, the $N_{\rm u}$-user signal-to-noise ratio at the output of the subcarrier filter is calculated in [8], as

$$SNR_{\rm out}(N_{\rm u}) = \frac{A_1^2 R_{\rm subcar}(0)}{2BT_{\rm f}\sigma_{\rm n}^2 + 2BT_{\rm f}\sigma_{\rm self}^2 \sum_{k=2}^{N_{\rm u}} A_k^2}\,. \tag{2}$$

where $R_{\rm subcar}(0)$ is the correlation function of the process $\widetilde{R}_w(d^{(1)}(u,t))$ evaluated at zero shift. The parameter B is a one-sided noise equivalent bandwidth of the subcarrier filter and $\sigma_{\rm n}^2$ is the variance of the receiver noise samples at the correlator output. The quantity $\sigma_{\rm self}^2$ is defined to be

$$\sigma_{\rm self}^2 \triangleq T_{\rm f}^{-1} \int_{-\infty}^{\infty} \left[\int_{-\infty}^{\infty} w_{\rm rec}(t+\zeta) w_{\rm cor}(t) dt \right]^2 d\zeta \,.$$

IV. The Digital Impulse Radio Multiple Access Receiver

A. Signal Processing for the DIRMA Receiver

The objective of the digital impulse radio multiple access (DIRMA) receiver is to determine a reasonable model for the signal processing necessary to demodulate one symbol of the transmission from the first transmitter with binary modulation. Specifically, $d_j^{(k)}(u) = \delta D^{(k)}_{\lfloor j/N_{\rm s} \rfloor}$ where the data sequence $\{D_i^{(k)}(u)\}_{i=-\infty}^{\infty}$ is a binary (0 or 1) symbol stream that conveys information in some form, and $N_{\rm s}$ is the number of monocycles per transmitted symbol. Here the notation $\lfloor x \rfloor$ denotes the integer part of x. As with the analog impulse radio, it is assumed that the receiver has perfectly achieved both clock and sequence synchronization for the signal transmitted by the first transmitter.

The optimal detection in a multi-user environment leads to complex receiver designs [9], [10]. However, if the number of users is large and no such multi-user detector is feasible, then it is reasonable to approximate the combined effect of the other users as a Gaussian random process [11], [7]. In this case, the optimum receiver is the correlation receiver [12], [13], which can be reduced to

$$\text{“decide } d_0^{(1)} = 0 \text{”} \quad \Longleftrightarrow \quad \underbrace{\sum_{j=0}^{N_{\rm s}-1} \overbrace{\int_{\tau_1+jT_{\rm f}}^{\tau_1+(j+1)T_{\rm f}} r(u,t) v(t-\tau_1-jT_{\rm f}-c_j^{(1)}T_{\rm c}) dt}^{\text{pulse correlator output } \triangleq\ \alpha_j(u)}}_{\text{test statistic } \triangleq\ \alpha(u)} \ > \ 0 \,, \tag{3}$$

where $v(t) \triangleq w_{\rm rec}(t) - w_{\rm rec}(t-\delta)$.

While the assumptions that make the rule in (3) optimal are not strictly valid, this decision rule will be used in the following to evaluate the performance of DIRMA receiver as a simple suboptimal means of making decisions because it is theoretically simple and suggests practical implementations. The statistic $\alpha(u)$ in (3) consists of summing the $N_{\rm s}$ correlations of the *correlator's template signal* $v(t)$ at various time shifts with the received signal $r(u,t)$. The signal processing corresponding to the decision rule in (3) is shown in Fig. 4. A graph of the template signal is shown in Fig. 5 using the typical received waveform given in Fig. 1.

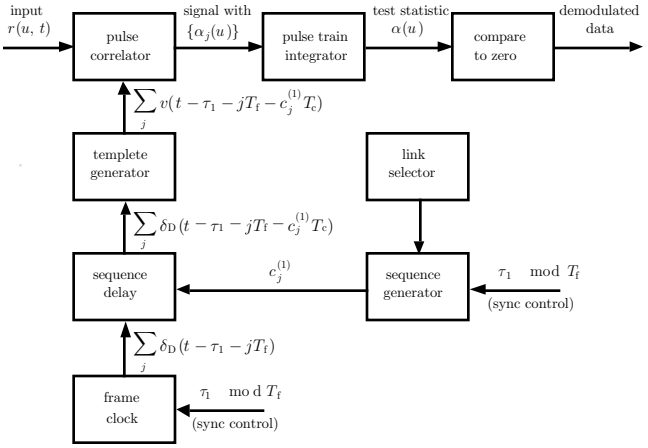

Fig. 4. Receiver block diagram for the reception of the first user's signal. Clock pulses are denoted by Dirac delta functions $\delta_{\rm D}(\cdot)$.

B. Signal-to-Noise Ratio of the DIRMA Receiver

The DIRMA receiver output signal-to-noise ratio is calculated in [11] as

$$SNR_{\rm out}(N_{\rm u}) = \frac{(N_{\rm s} A_1 m_{\rm p})^2}{\sigma_{\rm rec}^2 + N_{\rm s}\sigma_{\rm a}^2 \sum_{k=2}^{N_{\rm u}} A_k^2} \,, \tag{4}$$

where $\sigma_{\rm rec}^2$ is the variance of the receiver noise component at the pulse train integrator output. The parameters $m_{\rm p}$ and $\sigma_{\rm a}^2$ are defined to be

$$\begin{aligned} m_{\rm p} &= \int_{-\infty}^{\infty} w_{\rm rec}(x-\delta) v(x) dx, \qquad \text{and} \\ \sigma_{\rm a}^2 &= T_{\rm f}^{-1} \int_{-\infty}^{\infty} \left[\int_{-\infty}^{\infty} w_{\rm rec}(x-s) v(x) dx \right]^2 ds \,, \end{aligned}$$

respectively.

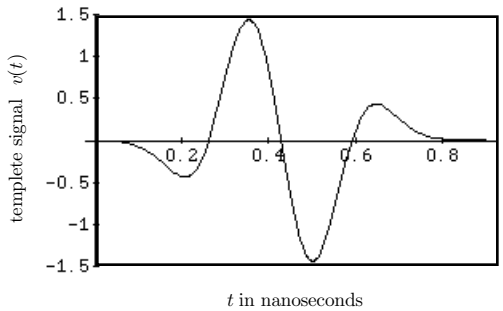

Fig. 5. The template signal $v(t)$ with the modulation parameter δ chosen to be 0.156 ns. Since the template is a difference of two pulses shifted by δ, the non-zero extent of the template signal is approximately δ plus the pulsewidth, i.e., about 0.86 ns.

V. Performance Measures of Multiple Access Systems

In this section, the interpretations of $N_{\rm u}$-user signal-to-noise ratio derived in the previous sections will be made and related to the performance of the impulse radio in terms of

multiple access capacity (MAC). Multiple access capacity is defined as the number of users that a multi-user communication system can support for a given level of uncoded bit error probability performance, data rate, and other modulation parameters.

The similarity of structure of the $SNR_{\rm out}(N_{\rm u})$ for AIRMA and DIRMA receivers given in (2) and (4), suggests a generalized expression of the form

$$SNR_{\rm out}(N_{\rm u}) = \left\{ SNR_{\rm out}^{-1}(1) + M \sum_{k=2}^{N_{\rm u}} \left(\frac{A_k}{A_1} \right)^2 \right\}^{-1} ,$$

where the parameter M for AIRMA and DIRMA receivers are given respectively by

$$M_{\rm AIRMA}^{-1} \triangleq \frac{R_{\rm subcar}(0)}{2BT_{\rm f}\sigma_{\rm self}^2} , \quad \text{and} \quad M_{\rm DIRMA}^{-1} \triangleq \frac{N_{\rm s} m_{\rm p}^2}{\sigma_{\rm a}^2} . \tag{5}$$

The $SNR_{\rm out}(N_{\rm u})$ can be interpreted as the required signal-to-noise ratio at the receiver demodulator to achieve a specified average bit error probability in the presence of the other $N_{\rm u}-1$ users. If only user 1 were active, then there would be no multiple access interference and the signal-to-noise ratio at the input of the receiver demodulator would increase to $SNR_{\rm out}(1)$. In this case the bit error probability would be clearly reduced from the specified value by as much as several orders of magnitude. Therefore the ratio of $SNR_{\rm out}(1)$ to $SNR_{\rm out}(N_{\rm u})$ represents the fractional increase in every transmitter's power required to maintain its signal-to-noise ratio, at a level equivalent to $SNR_{\rm out}(1)$ in its receiver, in the presence of multiple access interference caused by $N_{\rm u}-1$ other users. Therefore it is convenient to define the fractional increase in required power (in units of dB) as $\Delta P \triangleq 10\log_{10}\{SNR_{\rm out}(1)/SNR_{\rm out}(N_{\rm u})\}$.

Under the assumption of perfect power control, the number of users that multi-user communication system can support for a given data rate is shown in [8] to be

$$N_{\rm u}(\Delta P) = \left\lfloor M^{-1} SNR_{\rm out}^{-1}(N_{\rm u}) \left\{ 1 - 10^{-(\Delta P/10)} \right\} \right\rfloor + 1 ,$$

which is a monotonically increasing function of ΔP. Therefore

$$\begin{aligned} N_{\rm u}(\Delta P) &\le \lim_{\Delta P \to \infty} N_{\rm u}(\Delta P) \\ &= \left\lfloor M^{-1} SNR_{\rm out}^{-1}(N_{\rm u}) \right\rfloor + 1 \triangleq N_{\max} . \end{aligned} \tag{6}$$

This result states that the number of users at a specified bit error rate (BER) can not be larger than $N_{\max}$, no matter how large the power of each user's signal is. In other words, when the number of active users is more than $N_{\max}$, then the receiver can not maintain the specified level of performance regardless of the additional available power. Similar results for direct sequence code division multiple-access system can be found in [14].

VI. Performance Evaluation of Multiple Access Systems

The performance of the impulse radio multiple access receiver is evaluated using the two specific examples of modulation schemes giving in the following. A duration of the single symbol used in these examples is $T_{\rm s} = N_{\rm s} T_{\rm f}$. For a fixed frame (pulse repetition) time $T_{\rm f}$, the *symbol rate* $R_{\rm s}$ determines the number $N_{\rm s}$ of monocycles that are modulated by a given binary symbol, via the equation $R_{\rm s} = \frac{1}{T_{\rm s}} = \frac{1}{N_{\rm s} T_{\rm f}}$ sec^{-1}.

A. AIRMA Receiver Example

As an example for AIRMA receivers with analog subcarrier signaling, consider the frequency shift keyed (FSK) data modulation with,

$$d^{(k)}(u,t) = K \sum_n \lceil \overline{T_{\rm s}} \rceil (t - nT_{\rm s}) \cos[2\pi(f_{\rm c} + \Delta f_n(u))t + \theta(u)] .$$

The scaling constant K is chosen such that the data modulation levels are small enough that $d_j^{(1)}(u)$ always falls in the linear region and the approximation in (1) is reasonable. The random variable $\theta(u)$ is uniformly distributed on the interval $[-\pi, \pi)$. In the case of binary FSK, the carrier frequency $f_{\rm c}$ is shifted by $\Delta f_n(u) = f_0$ or $\Delta f_n(u) = f_1$ depending upon whether the $n^{\underline{\rm th}}$ data symbol is zero or one, respectively. For AIRMA receivers detecting analog FSK modulation with $K = 0.025$, $T_{\rm m} = 0.2877$ ns, $T_{\rm f} = 100$ ns, and the data rate $R_{\rm s} = 19.2$ kbps, $M_{\rm AIRMA}^{-1}$ is evaluated numerically as 4.63×10^4. In this calculation, the subcarrier filter bandwidth is set as $2B = 1/T_{\rm s}$.

B. DIRMA Receiver Example

As an example for DIRMA receivers with digital modulation, consider the binary pulse position modulation (BPPM). In DIRMA receivers the modulation parameter δ, which affects the shape of the template signal $v(t)$, appears only in $m_{\rm p}$ and $\sigma_{\rm a}^2$ implicitly, and can be adjusted to maximize $SNR_{\rm out}(N_{\rm u})$ under various conditions. When the receiver noise dominates the multiple-access noise, e.g., when there is only one user or when there is a strong external interferer, then it can be shown that the optimum choice of modulation parameter is that which maximizes $|m_{\rm p}|$, namely $\delta \approx 0.156$. On the other hand, when the receiver noise is negligible and $SNR_{\rm out}(1)$ is nearly infinite, then the optimum choice of δ, suggested by (4), is that which maximizes $|m_{\rm p}|/\sigma_{\rm a}$, namely $\delta \approx 0.144$. Little is lost in choosing either of these values, and δ is chosen to be $\delta = 0.156$ ns. When $\delta = 0.156$ and $T_{\rm f} = 100$ ns, then $m_{\rm p} = -0.1746$ and $\sigma_{\rm a}^2 = 0.006045$. In this case, the unitless constant that is required for calculating $M_{\rm DIRMA}^{-1}$ in (5) is $m_{\rm p}^2/\sigma_{\rm a}^2 \approx 504$. With the above choice of δ, $T_{\rm m} = 0.2877$ ns, and $R_{\rm s} = 19.2$ kbps, the parameter $M_{\rm DIRMA}^{-1}$ is calculated to be 2.63×10^5.

C. Performance Evaluation

The number of users versus additional required power for AIRMA and DIRMA receivers are plotted in Fig. 6 for typical BERs. To maintain BER of 10^{-3}, 10^{-4}, and 10^{-5} in a communications system with no error control coding, $SNR_{\rm out}(N_{\rm u})$ must be 12.8 dB, 14.4 dB, and 15.6 dB respectively. These curves are plotted using the parameters

described in previous section. Note that the number of users increase rapidly as the ΔP increases from 0 to 10 dB. However, this improvement becomes gradual as ΔP increases from 10 to 20 dB. After this point, only negligible improvement can be made as ΔP increases and finally reaches $N_{\max}$. In practice, impulse radios are expected to operate in regions where the increase in the number of users as a function of ΔP is rapid. It can be seen that the performance of DIRMA receivers in terms of multiple access capacity can be better than AIRMA receiver by more than a factor of 5. Furthermore, Fig. 6 quantitatively provides the trade-off between the number of additional users and the additional power required to maintain the respective BER. The value of $N_{\max}$ for AIRMA is calculated to be 4846, 3353, and 2544 for BERs of 10^{-3}, 10^{-4}, and 10^{-5}. Similarly $N_{\max}$ for DIRMA is calculated to be 27488, 19017, and 14426 for BERs of 10^{-3}, 10^{-4}, and 10^{-5}. The significance of (7) is also clear from Fig. 6, in that the number of users are less than $N_{\max}$.

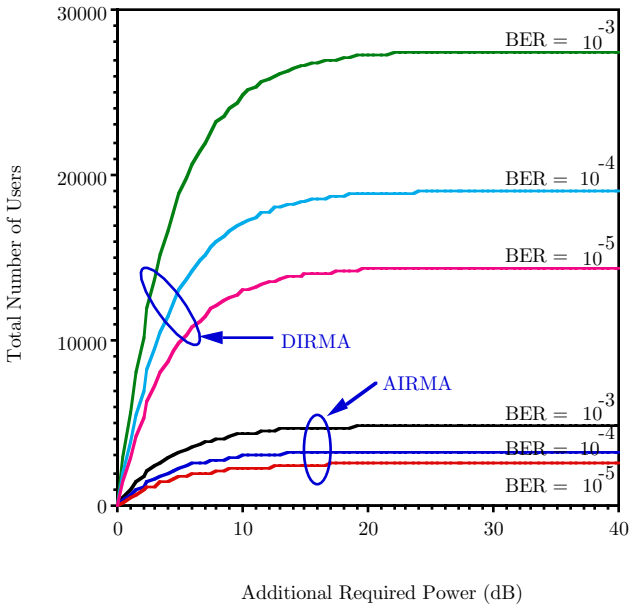

Fig. 6. Total number of users versus additional required power (dB) for AIRMA and DIRMA receivers. This figure is plotted for three different performance levels with the data rate of 19.2 Kbps.

VII. Conclusion

A Comparison of AIRMA and DIRMA receivers are made in terms of multiple access capacity under ideal propagation conditions. It is shown that each of the expressions for these two receivers have identical structure with the exception of the constant M which depends specifically on modulations parameters. The multiple access capacity is shown to initially increase rapidly as additional required power increases. However these improvements become gradual after a certain point and finally reach the limits which are referred to as maximum multiple access capacity. It is demonstrated that the performance of DIRMA receivers can be better than AIRMA receivers by more than a factor of 5. This can be attributed to the fact that the AIRMA receiver's subcarrier power is limited by the linear region of the cross correlation function between the received monocycle waveform and the template generator output; where as the modulation parameter δ is optimized for the DIRMA receiver to maximize the signal-to-noise ratio. The results obtained in this paper are quite general and quantitatively provide the trade-off for system design issues.

Acknowledgments

The authors wish to thank Mark Barnes, Glenn Wolenec, Ivan Cowie, and Larry Fullerton of Time Domain Systems, and Paul Withington of Pulson Communications for several helpful discussions concerning the technology, capabilities, and signal processing of impulse signals.

References

[1] M. K. Simon, J. K. Omura, R. A. Scholtz, and B. K. Levitt, *Spread Spectrum Communications Handbook*. McGraw-Hill, Inc., revised ed., 1994.

[2] R. L. Peterson, R. E. Ziemer, and D. E. Borth, *Introduction to Spread Spectrum Communications*. Englewood Cliffs, New Jersey 07632: Prentice Hall, first ed., 1995.

[3] M. Z. Win and R. A. Scholtz, "Characterization of ultra-wide bandwidth wireless indoor communications channel: A communications theoretic view," *IEEE Trans. Commun.*, July 1997. submitted.

[4] M. Z. Win, R. A. Scholtz, and M. A. Barnes, "Ultra-wide bandwidth signal propagation for indoor wireless communications," in *Proc. IEEE Int. Conf. on Comm.*, pp. 56–60, June 1997. Montréal, Canada.

[5] M. Z. Win, F. Ramirez-Mireles, R. A. Scholtz, and M. Barnes, "Ultra-wide bandwidth (UWB) signal propagation for outdoor wireless communications," in *Proc. 47th Annual Int. Veh. Technol. Conf.*, pp. 251–255, May 1997. Phoenix, AZ.

[6] M. Z. Win and R. A. Scholtz, "Design of ultra-wide bandwidth Rake receiver for time-hopping SSMA impulse radio and its application to wireless indoor multipath communications," *to be submitted to IEEE Trans. Commun.*, 1997. in preparation.

[7] M. Z. Win, R. A. Scholtz, and L. W. Fullerton, "Time-hopping SSMA techniques for impulse radio with an analog modulated data subcarrier," in *Proc. IEEE Fourth Int. Symp. on Spread Spectrum Techniques & Applications*, pp. 359–364, Sept. 1996. Mainz, Germany.

[8] M. Z. Win and R. A. Scholtz, "Ultra-wide bandwidth (UWB) time-hopping spread-spectrum impulse radio for wireless multiple access communications," *IEEE Trans. Commun.*, Jan. 1997. submitted.

[9] H. V. Poor, "Signal processing for wideband communications," *IEEE Information Society Newsletter*, June 1992.

[10] S. Verdu, "Recent progress in multiuser detection," in *Multiple Access Communications: Foundations for Emerging Technologies*, pp. 164–175, IEEE Press, 1993.

[11] R. A. Scholtz, "Multiple access with time-hopping impulse modulation," in *Proc. MILCOM*, Oct. 1993.

[12] J. M. Wozencraft and I. M. Jacobs, *Principles of Communication Engineering*. London: John Wiley & Sons, Inc., first ed., 1965.

[13] M. K. Simon, S. M. Hinedi, and W. C. Lindsey, *Digital Communication Techniques: Signal Design and Detection*. Englewood Cliffs, New Jersey 07632: Prentice Hall, first ed., 1995.

[14] C. L. Weber, G. K. Huth, and B. H. Batson, "Performance considerations of code division multiple-access systems," *IEEE Trans. on Vehicul. Technol.*, vol. VT-30, pp. 3–9, Feb. 1981.